

PNAS

www.pnas.org

Supplementary Information for

Cell adhesion signals regulate the nuclear receptor activity

Kotaro Sugimoto, Naoki Ichikawa-Tomikawa, Korehito Kashiwagi, Chihiro Endo,
Satoshi Tanaka, Norimasa Sawada, Tetsuya Watabe, Tomohito Higashi, Hideki Chiba

Hideki Chiba

Email: hidchiba@fmu.ac.jp

This PDF file includes:

Supplementary text
Figures S1 to S12
Tables S1 to S3
SI References

Materials and methods

Antibodies

The antibodies used in this study are listed in Supplementary Table S1.

Cell culture, plasmids and cell lines

F9 L32T2 cells, which constitutively expresses both doxycycline (Dox)-controlled transactivator rtTA and 4-hydroxy tamoxifen (OHT)-dependent Cre recombinase Cre-ER^T (56), F9 L32T2:*HNF4α* cells (also known as F9:*iHNF4α* cells) (25), F9:*Rxra*^{-/-}:*Rarg*^{-/-} (31, 32), and F9:*Cldn6* (28) and F9 L32T2:*Cldn6* cells (also known as F9:*iCldn6*) (28) were generated as described previously. F9:*HA-Cldn6*, F9:*HA-Cldn6ΔC1/2* (deletion of residues 202-219), and F9:*HA-Cldn6ΔC* (deletion of residues 189-219), F9:*iCldn6-Flag*, F9:*iCldn6ΔEC1-Flag* (deletion of residues 34-76), F9:*iCldn6ΔEC2-Flag* (deletion of residues 143-155), F9:*Cldn6Y196A*, F9:*Cldn6Y200A*, F9:*Cldn6Y213A*, and F9:*Cldn6Y218A* cell lines were established by transfection with corresponding expression vectors into F9 L32T2 cells by electroporation.

F9:*Rxra*^{-/-}:*Rarg*^{-/-}:*Cldn6*, F9:*Rxra*^{-/-}:*Rarg*^{-/-}:*Cldn6:iRxra-Rarg2* and its mutants (-*Rarg2ΔN* [deletion of residues 1-75], -*Rarg2ΔC* [deletion of residues 152-448], -*Rarg2S192A*, -*Rarg2S360A*, -*Rarg2S379A*, -*Rarg2T388A*, -*Rarg2S426A/S427A*), F9:*Rxra*^{-/-}:*Rarg*^{-/-}:*iRxra-Rarg2*, F9:*Rxra*^{-/-}:*Rarg*^{-/-}:*iRxra-Rarg2S360E*, and F9:*Rxra*^{-/-}:*Rarg*^{-/-}:*iRxra-Rarg2S379E* cells were generated in an analogous manner transfecting into F9:*Rxra*^{-/-}:*Rarg*^{-/-} cell line. Cells were plated in DMEM with 10% FBS, and the medium was changed every two days. They were treated with 1 μg/ml of Dox, 0.2 or 1 μM of C-CPE, 1-100 μM of PP2 (Calbiochem), 1-100 μM of other SFK inhibitors (Src Family Inhibitor Set, Biaffin), 10 μM of LY294200, or 10 μM of AKT inhibitor VIII (funakoshi), 100 ng/ml of human IGF-1 (funakoshi), 100 ng/ml of mouse EGF (funakoshi), 1-1,000 ng/ml of all trans retinoic acid (Sigma) one or two days after plating. Stealth Select siRNAs synthesized by Invitrogen were transfected using Lipofectamine RNAiMAX (Thermo Fisher Scientific). The sequences are shown in Supplementary Table S2. For preparation of charcoal-treated FBS, 500 ml of FBS was treated with 0.5 g of Charcoal, dextran coated (Sigma) overnight at 4°C followed by filtration using 0.22 μm cellulose acetate filter membranes. XTT assay was performed using cell proliferation kit II (Roche Applied Science).

HEK293T and MCF-7 cells were maintained in DMEM with 10% FBS. For transient expression of the target genes (*CLDN6* and *Flag-Rxra-HA-Rarg2*), 5×10⁶ cells were transfected with 10 μg of the indicated vectors using 30 μg of Polyethylenimine Max (PEI Max, Cosmo Bio)

8 h after passage. Lentiviral vectors (*CLDN4*, *CLDN6*, *HA-ESR1*, *HA-ESR1S518E*) were generated by transfecting HEK293T cells with 10 µg of the lentiviral transfer plasmids modified from CSII-EF-MCS-IRES2-Venus (RIKEN, RDB04384), 5 µg of packaging plasmids psPAX2 (Addgene, #12260) and pCMV-VSV-G-RSV-Rev (RIKEN, RDB04393) using PEI Max. Culture media containing recombinant lentiviruses were collected 72 h after transfection. The lentiviral vectors were added to cell culture medium after filtration. More than 48 h after transfection, the MCF-7 cells were used for further analysis. 1 µM of Estradiol (Sigma), 100 ng/ml of human IGF-1 (funakoshi), and 100 ng/ml of mouse EGF (funakoshi) was treated one day after passage.

Mouse ES cells were provided from RIKEN BioResource Center Cell Bank (Cell No. AES0008). They were cultured on SNL 76/7 feeder cells (Sigma) in DMEM (high glucose and 1 mM sodium pyruvate) supplemented with 15% KnockOut serum replacement (Gibco), 0.1 mM 2-mercaptoethanol (Sigma), 1,000 U/ml leukemia inhibitory factor (Wako), 0.1 mM nonessential amino acids (Gibco), and GlutaMAX solution (Gibco).

The morphology of these cells was checked by phase-contrast microscopy (Axiovert 200 and HAL100, Carl Zeiss).

Embryoid formation

For embryoid body (EB) formation, 6×10^6 ES cells were first cultured on gelatin-coated 10 cm-culture dishes without feeder cells for three days in the same medium, and subjected to suspension culture in three 10 cm-bacterial dishes in the DMEM with 20% FBS, 0.1 mM 2-mercaptoethanol (Sigma), 0.1 mM nonessential amino acids (Gibco), and GlutaMAX solution (Gibco). The medium was changed every other day. The lentiviral vectors and inhibitors were added one day after being shifted to the suspension culture.

C-CPE construction and purification

The expression vector pET16b coding C-CPE194-319 (57) was kindly provided by Dr. M. Kondoh (Osaka University) (58). *E. coli* BL21 (DE3, which was with the vector was grown at room temperature, and protein expression was stimulated by the addition of isopropyl-1-thio-β-D-galactoside, followed by purification using TALON His purification resin (Clontech).

Immunoprecipitation and immunoblot

Immunoprecipitation (Fig. 2A,B; Fig. 3B; Fig. 5C,D) was performed using an Immunoprecipitation kit (Protein G, Sigma), following the manufacturer's protocol. For crosslinking-immunoprecipitation (Fig. 2F-H), the cells were homogenized in lysis buffer (20

mM HEPES, 150 mM NaCl, 10% glycerol, 1% NP-40, protease inhibitor mixture cocktail mini [Roche Applied Science], 1 mM Na₃VO₄, and 2 mM NaF, pH 7.4) at 4°C for 30 min. To cross-link antibodies to protein A sepharose beads (CL-4B, GE Healthcare), dimethylpimelimidate (DMP) was added to boracic acid. The cell lysate incubated with the beads and bound protein was eluted with 0.1 M glycine-HCl (pH2.0). Phos-tag SDS-PAGE was performed using SuperSepTM Phos-tagTM (50 μmol/l), 12.5%, 17 well-precast gel (FUJIFILM) following the manufacturer's protocol. Immunoblot analysis was performed as previously described (27, 59). A Can Get Signal Immunoreaction Enhancer Solution kit (TOYOBO) was used for ZO-1α+, FLAG-tag, HA-tag, and pSFK detections. Each blot was stripped with Restore Western blot stripping buffer (Pierce Chemical) and immunoprobed with anti-actin antibody. Signals in the immunoblots were quantified using ImageJ software (Wayne Rasband National Institutes of Health). The protein levels were normalized to the corresponding actin levels, and their relative levels were then presented.

Immunohistochemistry

F9 cells were grown on coverslips coated by Cellmatrix Type I-A (Nitta gelatin). EBs were concentrated in conical tubes by gravity flow and embedded in NEG50 compound (Richard-Allan Scientific). After being frozen, they were cut into 8-μm thin slice. These samples were fixed in 4% paraformaldehyde for 10 min at room temperature. After washing with PBS, the samples were preincubated in PBS containing 5% skimmed milk. They were subsequently incubated overnight at 4°C with primary antibodies in PBS, then rinsed again with PBS, followed by a reaction for 1 h at room temperature with appropriate secondary antibodies. All samples were examined using a laser-scanning confocal microscope (FV1000, Olympus). Photographs were processed with Photoshop CS5 (Adobe) and ImageJ software (Wayne Rasband National Institutes of Health).

Chromatin immunoprecipitation

Chromatin immunoprecipitation (ChIP) was performed using SimpleChIP Plus Enzymatic Chromatin IP Kit (Agarose Beads, Cell Signaling Technology) following the manufacturer's protocol. Purified DNA was amplified by PCR with primers listed in Supplementary Table 3 and GoTaq Green Master Mix (Promega).

RT-PCR analysis

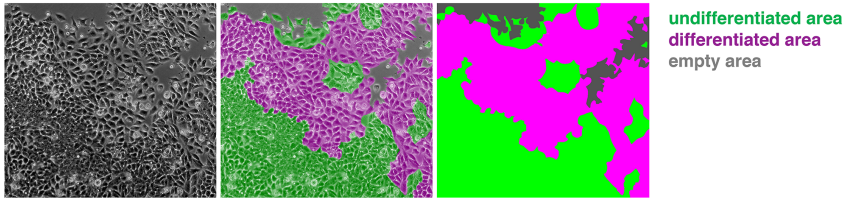
For analysis of gene expression, total RNA was isolated from cells using TRIzol RNA Isolation Reagents (Thermo Fisher Scientific), and reverse transcription was performed using Primescript II RT Kit (Clontech). For PCR, the target sequences were amplified using GoTaq Green Master Mix (Promega). The PCR primers and conditions are indicated in Supplementary Table S3.

Aliquots of the PCR products were loaded onto 2.5% agarose gel and analyzed after staining with ethidium bromide. Quantitative PCR (qPCR) was performed using THUNDERBIRD SYBR qPCR Mix (TOYOBO) and Step One Real-Time PCR System (Applied Biosystems).

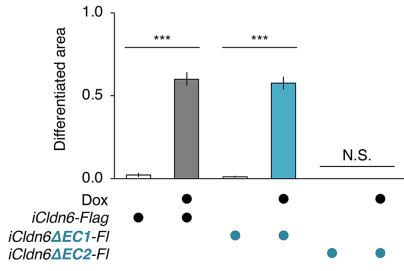
Statistical analysis

For quantitative analysis of F9 cell morphology, differentiated and undifferentiated cells were marked in ten or twenty non overlapping fields from six plates using Photoshop CC software (Adobe, Fig. S1A). The pixel number of differentiated cell areas was divided by the pixel number of differentiated and undifferentiated areas to determine occupancy of differentiated cells. The relative differentiated areas were presented as mean \pm SD from ten or twenty fields. The XTT assay values are presented as the mean + SD from three samples, and statistical significances were analyzed by paired sample two-tailed *t*-test. The PCR values are presented as the mean \pm SD from three or four samples. Original values were quantified by ImageJ software (Wayne Rasband National Institutes of Health). The expression levels of the target genes in RT-PCR were divided by the corresponding 36B4 signal intensity. Their relative levels were analyzed by paired sample two-tailed *t*-test to evaluate statistical significances. The proportion of categorized EBs (n=100) in each group was subjected to chi-square test, and their *p* values were calculated.

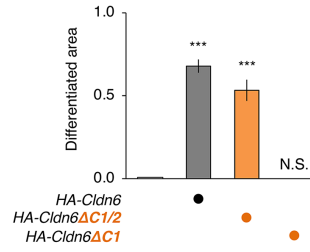
A



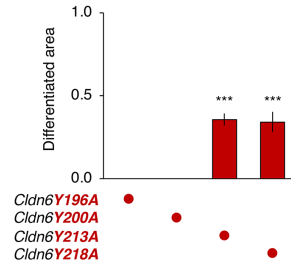
B



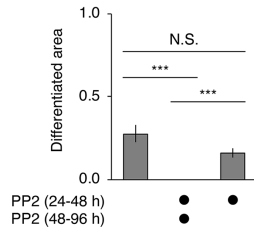
C



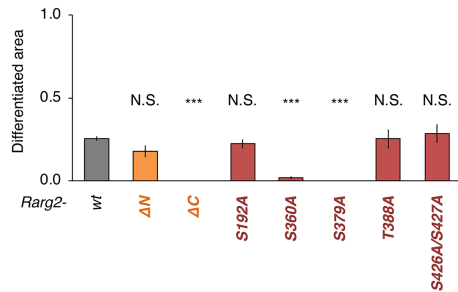
D



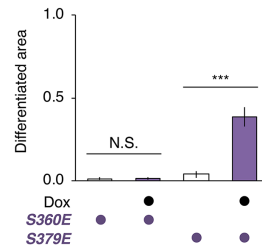
E



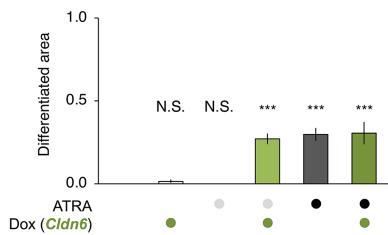
F



G



H



I

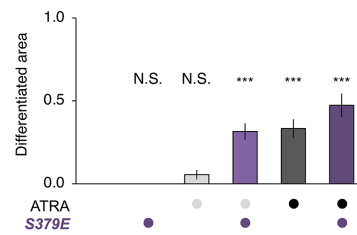


Fig. S1. Quantification of morphological differentiation in F9 stem cells. (A) Representative quantification of epithelial differentiation. (B-I) Proportion of the differentiated areas in the indicated F9 cells. F9:*iCldn6* cells were treated for 72 h with the vehicle or 1.0 $\mu\text{g/ml}$ Dox. F9:*Rxra*^{-/-}:*Rarg*^{-/-}:*iRxra-Rarg2S379E* cells were exposed for 72 h to 1.0 $\mu\text{g/ml}$ Dox, ATRA (1 nM or 1,000 nM) or both together (H,I). The relative differentiated areas are shown in the histograms (mean \pm SD) from twenty (B) and ten fields (C-I). *** $P < 0.001$; N.S., not significant.

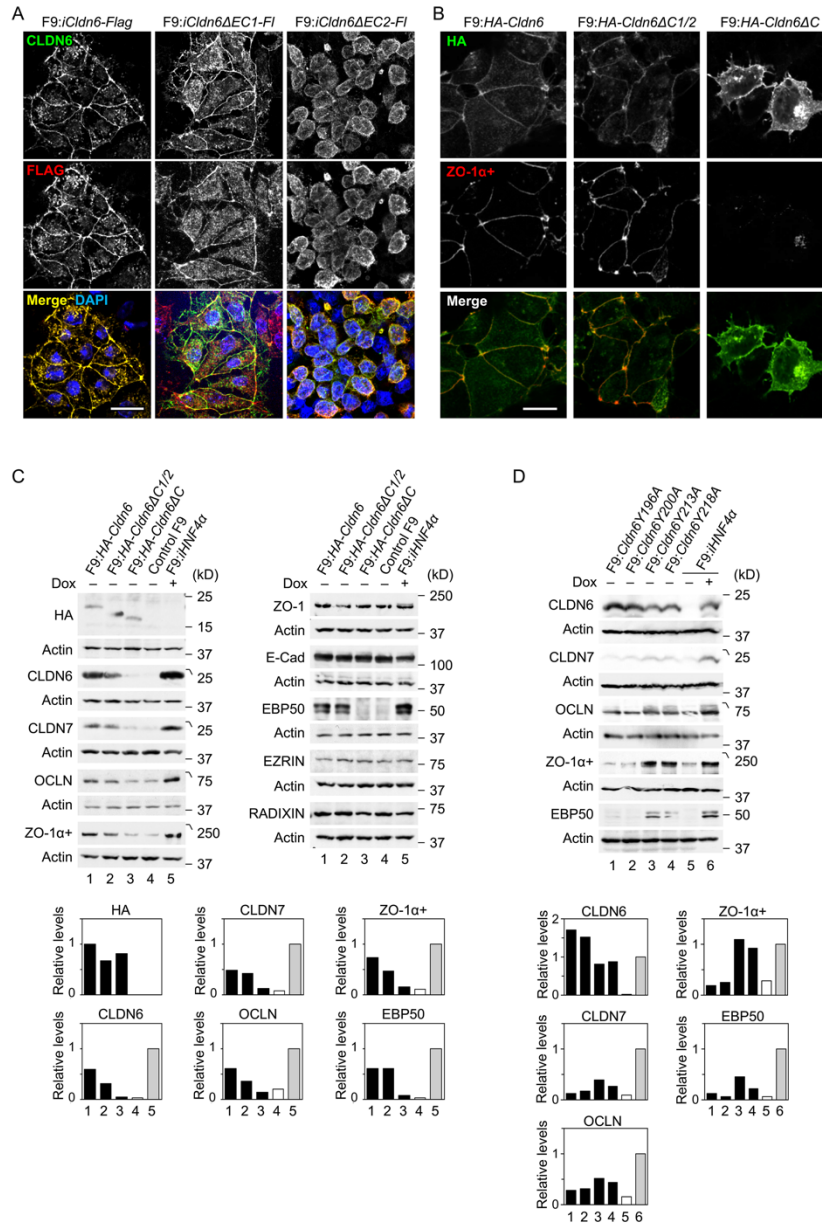


Fig. S2. The EC2 and C-terminal cytoplasmic domains of CLDN6 are required for their signaling property. (A,B) Confocal images of the revealed cells stained for the indicated markers. F9:*iCldn6-Flag*, F9:*iCldn6ΔEC1-Flag* and F9:*iCldn6ΔEC2-Flag* cells were treated for 72 h with either the vehicle or 1.0 μg/ml doxycycline (Dox). Scale bars, 20 μm. (C,D) Western blot for the indicated proteins in the revealed cell lines. F9:*iHNF4α* cells were treated for 72 h with the vehicle or 1.0 μg/ml doxycycline (Dox). Quantification of the protein levels is shown in the histograms.

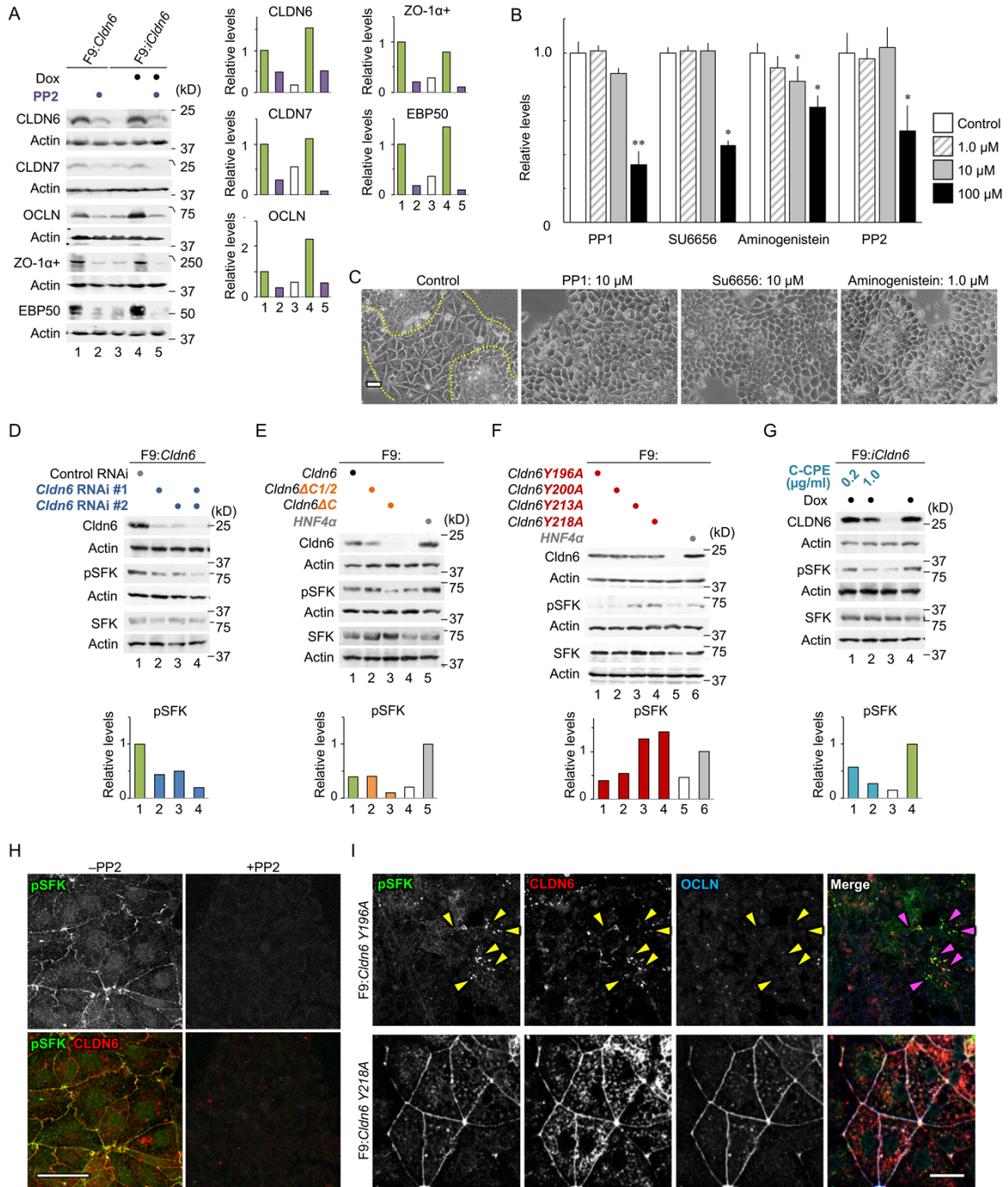


Fig. S3. SFKs are involved in the CLDN6-triggered signaling. (A) Western blot for the indicated proteins in F9:*Cldn6* and F9:*iCldn6* cells grown in the presence or absence of 10 μ M PP2. F9:*iCldn6* cells were treated for 72 h with 1.0 μ g/ml doxycycline (Dox). Quantification of the protein levels is shown in the histograms. (B,C) Effect of several SFK inhibitors on cell viability (B) and morphological appearance (C) of F9:*Cldn6* cells. Quantification of cell viability (mean + SD; $n = 3$) is shown in the histograms. * $P < 0.05$; ** $P < 0.001$. The boundaries between undifferentiated and epithelial cells are shown in the dashed yellow lines. (D-G) Western blot for the indicated proteins in various F9 cells. F9:*iCldn6* cells were grown for 72 h in the presence or absence of 1.0 μ g/ml doxycycline (Dox) and either 0.2 μ g/ml or 1.0 μ g/ml C-CPE. F9:*iHNF4 α* cells were treated for 72 h with the vehicle or 1.0 μ g/ml Dox. Quantification of the pSFK levels is shown in the histograms. (H) Confocal images of vehicle- and PP2-treated F9:*Cldn6* cells stained for the indicated markers. (I) Confocal images of the revealed F9 mutants stained for the indicated markers. The arrowheads indicate the recruitment of pSFK to CLDN6-positive primordial cell junction of undifferentiated cells. Scale bars, 20 μ m.

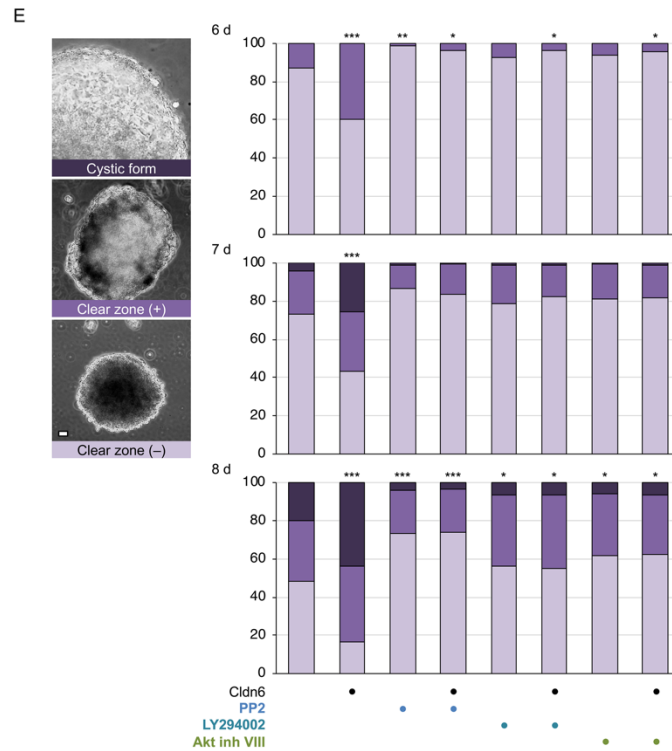
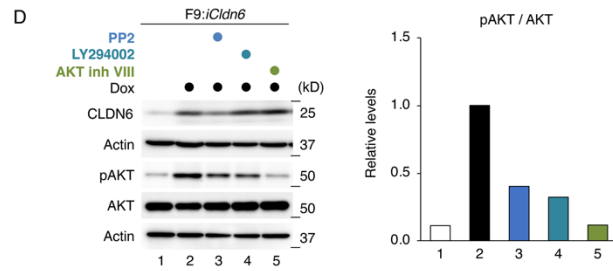
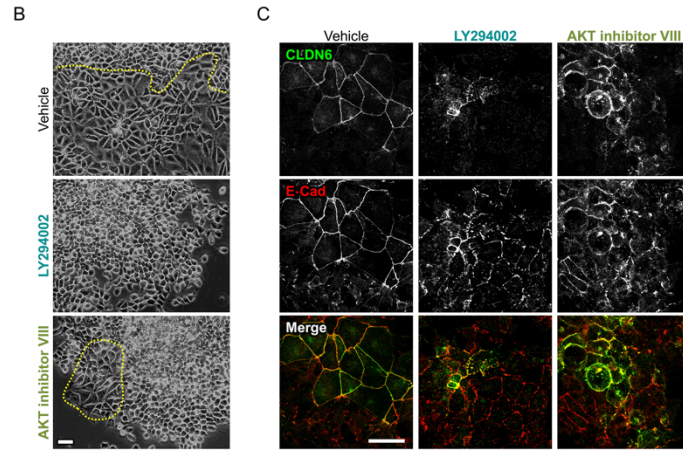
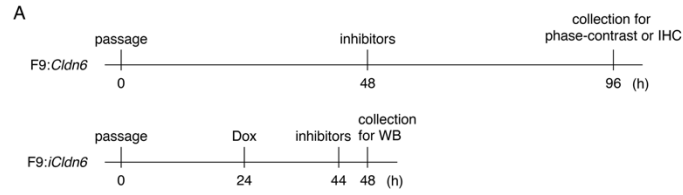


Fig. S4. The PI3K/AKT cascade contributes to the CLDN6/SFK-induced signaling. (A) F9:*Cldn6* and F9:*iCldn6* cells were grown as in the indicated culture condition. (B-D) Effects of PI3K and AKT inhibitors (LY294002 and AKT inh VIII, 10 μ M) on morphological appearance (B), mature cell-cell junction formation (C) and the AKT activity (D). The borders between undifferentiated and epithelial cells are shown in the dashed yellow lines. Quantification of the protein levels is shown in the histograms. (E) Left, the three forms of the appearance of EBs. Right, mouse ES cells were transfected with mock or CLDN6 expression vectors, and EBs were cultured for eight days in the presence or absence of the indicated inhibitors, followed by categorization of their morphological appearance. Solid form was classified to clear zone (+) and clear zone (-). All values were compared with those in control values. * P <0.05; ** P <0.01; *** P <0.001. Scale bars, 20 μ m.

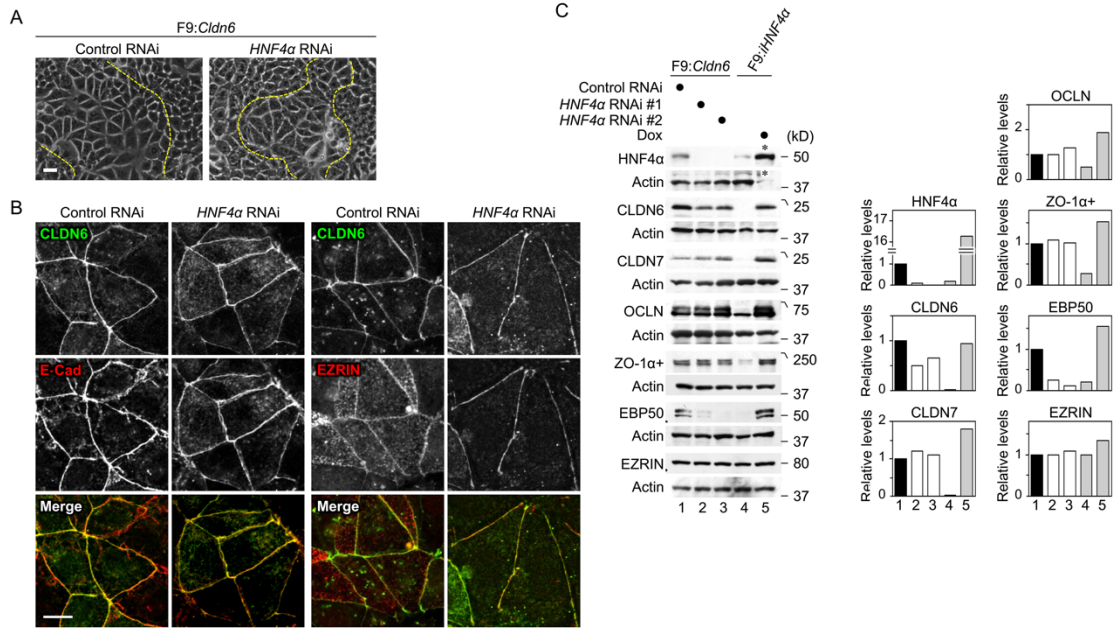


Fig. S5. The HNF4 α does not directly participate in the CLDN6-initiated epithelial signaling. (A) Effect of HNF4 α knockdown on morphological appearance of F9:*Cldn6* cells. The boundaries between undifferentiated and epithelial cells are shown in the dashed yellow lines. (B) Effect of HNF4 α suppression on confocal images of F9:*Cldn6* cells stained for the indicated markers. (C) Effect of HNF4 α knockdown on Western blot for the indicated proteins in F9:*Cldn6* cells. F9:*HNF4α* cells were treated for 72 h with either the vehicle or 1.0 μ g/ml doxycycline (Dox). The asterisks indicate that 10% amount were applied in Lane 5 compared with Lanes 1–4. Quantification of the protein levels is shown in the histograms. Scale bars, 20 μ m.

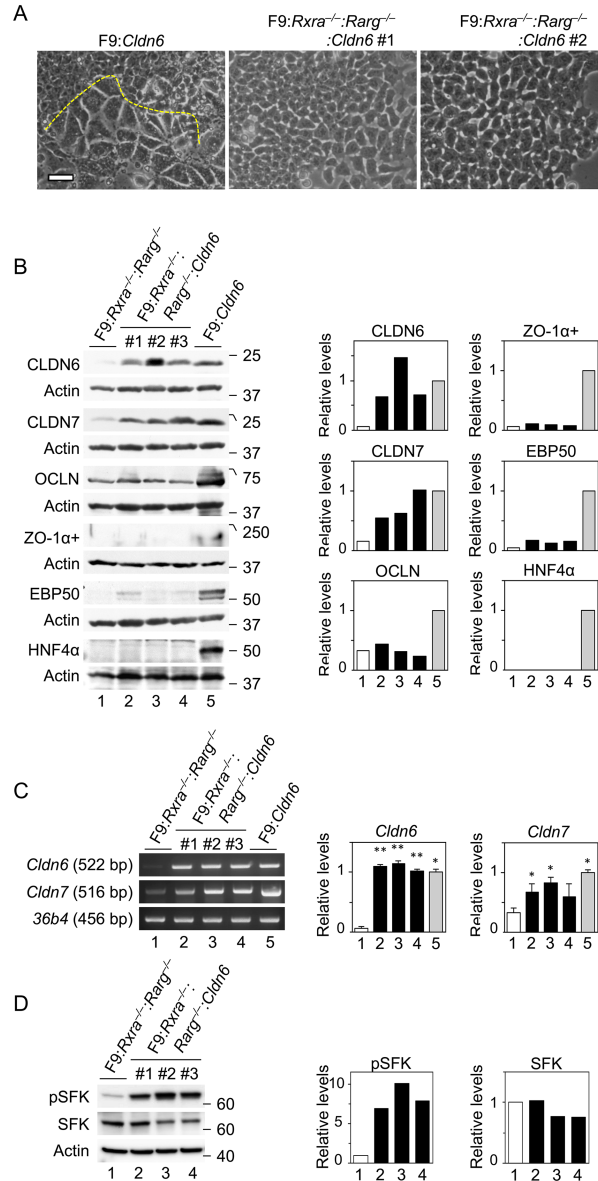


Fig. S6. The CLDN6-adhesion signaling targets retinoid receptors. (A) Morphological appearance of F9:*Cldn6* and F9:*Rxra*^{-/-}:*Rarg*^{-/-}:*Cldn6* cells. The borders between undifferentiated and epithelial cells are shown in the dashed yellow lines. Scale bar, 20 μ m. (B,D) Western blot for the indicated proteins in the revealed F9 cells. (C) RT-PCR for the indicated molecules in various F9 cells. Quantification of the protein and mRNA (mean + SD; $n = 3$) levels is shown in the histograms. * $P < 0.05$; ** $P < 0.001$.

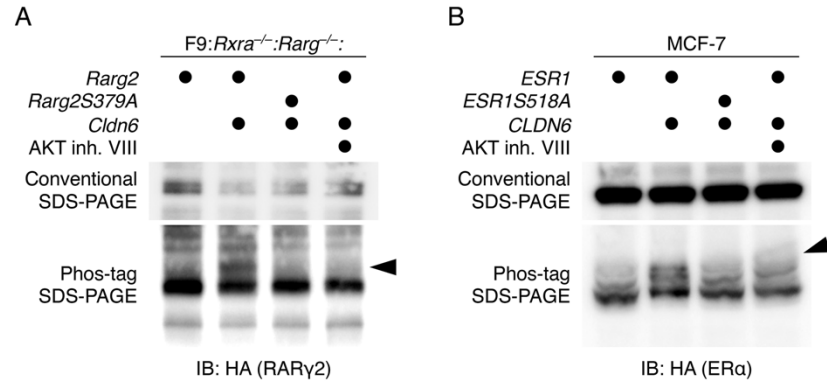


Fig. S7. The CLDN6/AKT axis phosphorylates RAR γ and ER α . (A,B) Phos-tag SDS-PAGE and subsequent immunoblot analysis indicates phosphorylation (arrowhead) of RAR γ and ER α in the indicated cells.

Fig. S8. RAR γ -S379 is involved in releasing NCoR. (A) The putative and established RA response elements (RAREs) in the promoters of *Rarb*, *Hnf4* and *Cldn6* genes are indicated in squares (dark and light reds, NCoR is strongly and moderately dissociated; dark grays, no effect on NCoR releasing, light grays, no NCoR binding). (B) Representative ChIP assay for NCoR-binding in the indicated F9 cells. Several RAREs in revealed target genes are numbered from the side close to the transcription start sites. Lower, quantification of relative NCoR-binding is shown in the histograms (mean \pm SD; $n = 3$). * $P < 0.05$; ** $P < 0.01$; *** $P < 0.001$. (C) Representative ChIP assay for RXR α /RAR γ -binding in the indicated F9 cells.

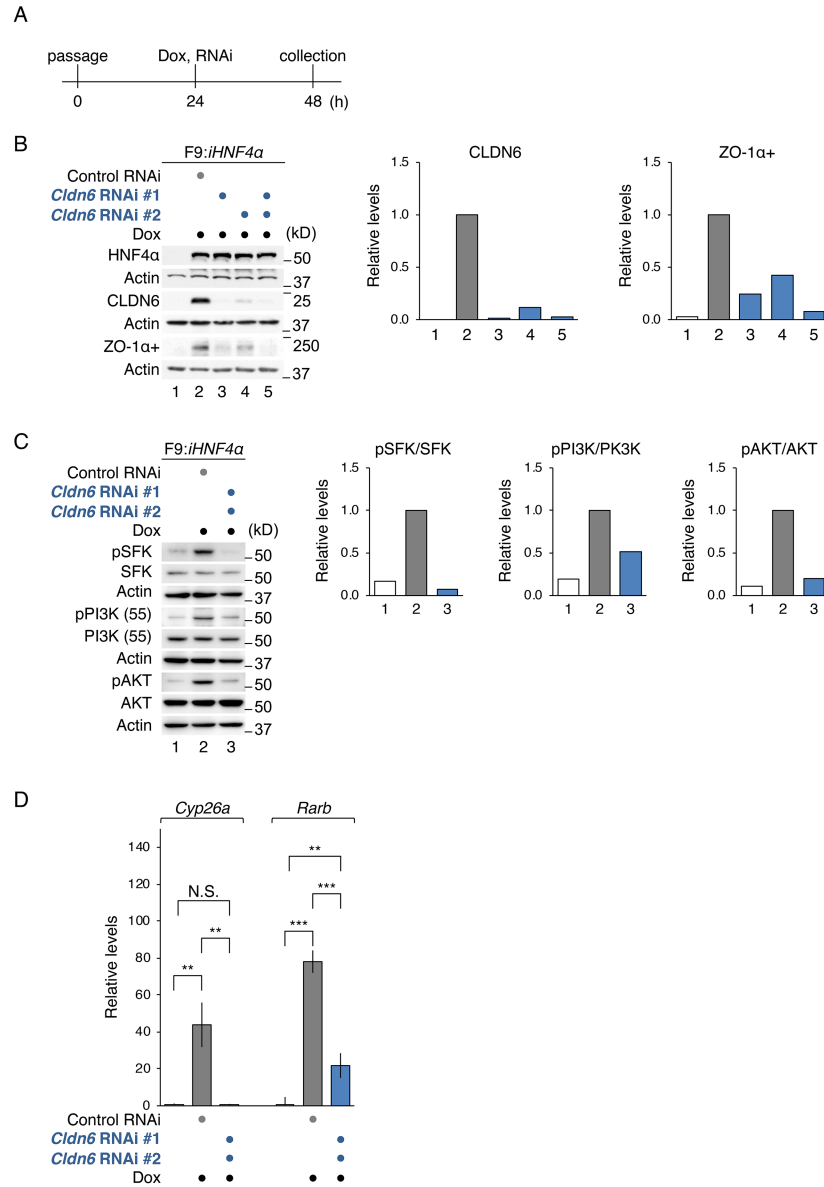


Fig. S9. CLDN6 knockdown prevents activation of SFK/PI3K/AKT and RAR target gene expression. (A) F9:*iHNF4α* were grown as in the indicated culture condition. (B,C) Western blot for the indicated proteins in the cells transfected with negative control siRNA or two distinct siRNAs against *Cldn6*. Quantification of the protein levels is shown in the histograms. (D) Quantitative RT-PCR for the indicated genes. The relative expression levels are shown in the histograms (mean \pm SD; $n = 4$). ** $P < 0.01$; *** $P < 0.001$; N.S., not significant.

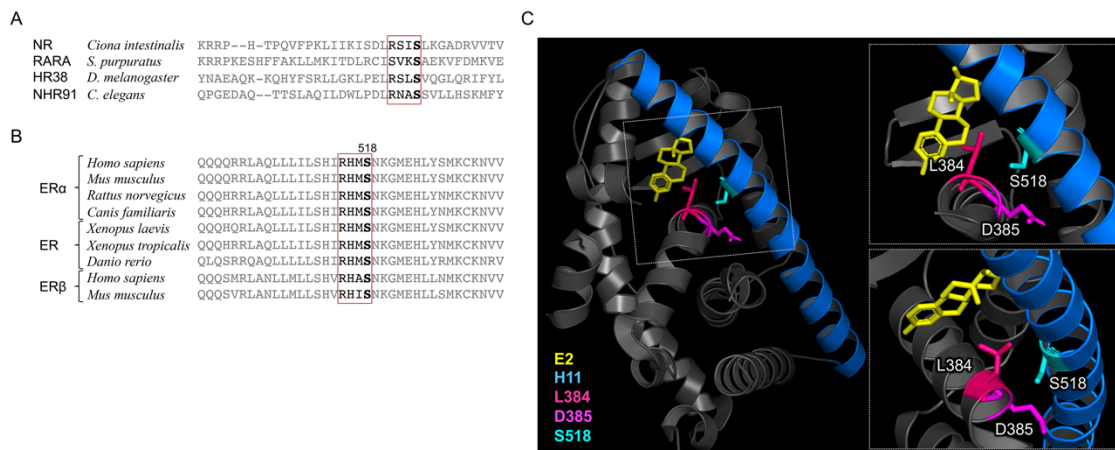


Fig. S10. Species conservation of the AKT-consensus phosphorylation motif in nuclear receptors and schematic representation of the holo-LBD of human ER α . (A,B) The AKT phosphorylation site is conserved among RARs and the closely related nuclear receptors in invertebrates (A), as well as among ERs in vertebrates (B). The conserved serine residues and AKT-consensus phosphorylation motif (RXXS, aa 515-518 for human ER α) are indicated in bold and red rectangle lines, respectively. (C) The structure of the holo-LBD of human ER α (60) was visualized by PyMOL.

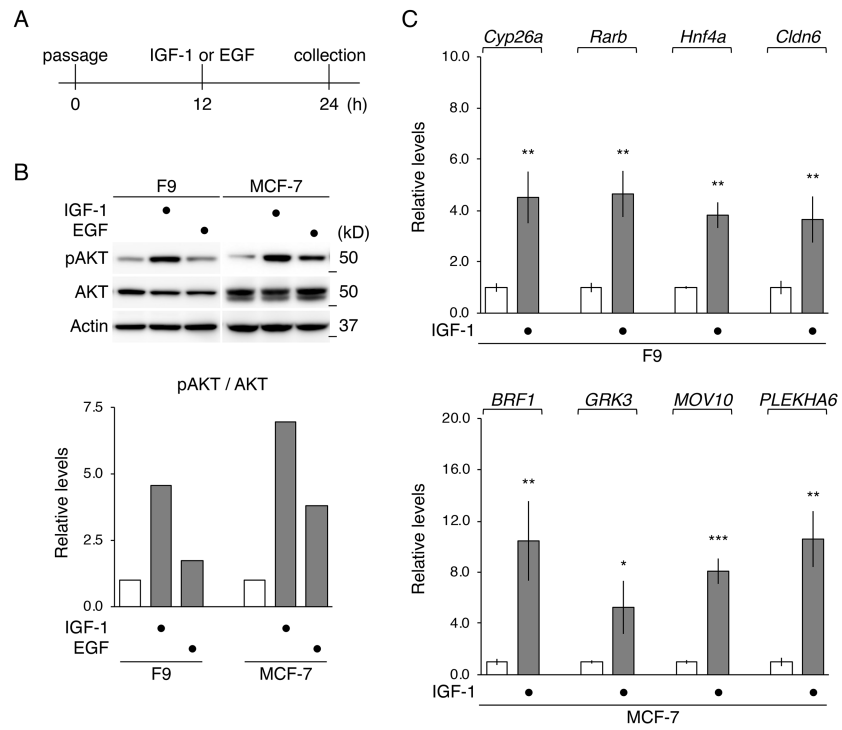


Fig. S11. IGF-1 activates AKT and induces the expression of RAR and ER target genes. (A) F9 and MCF-7 cells were cultured as in the indicated culture condition. (B) Western blot for the indicated proteins in the cells treated with the vehicle, 100 ng/ml IGF-1 or 100 ng/ml EGF. Quantification of the protein levels is shown in the histograms. (C) Quantitative RT-PCR for the indicated genes. The relative expression levels are shown in the histograms (mean \pm SD; $n = 4$). * $P < 0.05$; ** $P < 0.01$; *** $P < 0.001$.

A

```

CLDN1 -----SCSCP--RKTTSYPT-----PRYPKPTP
CLDN7 -----SCSCPGESEKAAAYRA-----PRSYPK--S
CLDN3 -----CCSCPDRKYAPTKE-----LYSAPRSTG
CLDN4 -----CCSCPFRSNDKPYSA-----KYSAARSVP
CLDN18 -----VMMCIACR-----GLTPDDSK
CLDN24 -----HCAACSSPAPAASSHY-----AGAGPRDHG
CLDN20 -----ISGVIFCTSYIQKNQEPWIY-----PPKQKLSTT
CLDN22 -----ISGVIFCTSYIQKNQEPWIY-----PPKQKLSTT
CLDN2 -----CFSCSPQGNRTNYD-----GYQAQPLAT
CLDN8 -----FCCVFCCTERSNSYRYSVPS-----HRTTQRSFH
CLDN17 -----CGYCCNRKERWHRYVPVA-----YRVQKDNQ
CLDN9 -----CCTCPPSHFERPRGP-----RLGYSIPSR
CLDN5 -----MCGGGLVCCGAWVCTGRPEFSF-----PVKYSAPRR
CLDN23 GFSLALSFAPWCEERCRCRKAPPAGPRRSSISTVYVDWPEPALTPAIKYSDGQHRPPP
CLDN6 -----CCACSSGGTQGPRHY-----MACYSTSVPHS
CLDN10 -----CFSISDNNKTPRMGYTYN-----GPTSAMSSR
CLDN12 -----FVWYACKSLSSPFWQPLYS-----HAPGMHTYSQP
CLDN13 -----CVNIPVCRDFPRCI-----ETPSARPSG
CLDN11 --ALCAIVATIWFVCAHREITIVSPGYSLYAGWIGAVMCLVGGCVIVCCSGDAQSFGEN
CLDN14 -----CLSCQDEAPYRPPQSRAG-----ATTTATAPAYRPP
CLDN19 -----CCTCPEPERANSIPQPYRSG-----PSTAAREPV
CLDN15 ---SILGGICVFSTCCSSKEEPATRAGLP-----YKPSTVVIPRA
CLDN16 -----CCLYLFKDVGPERNYP-----YAMRKPYSTA

```

B

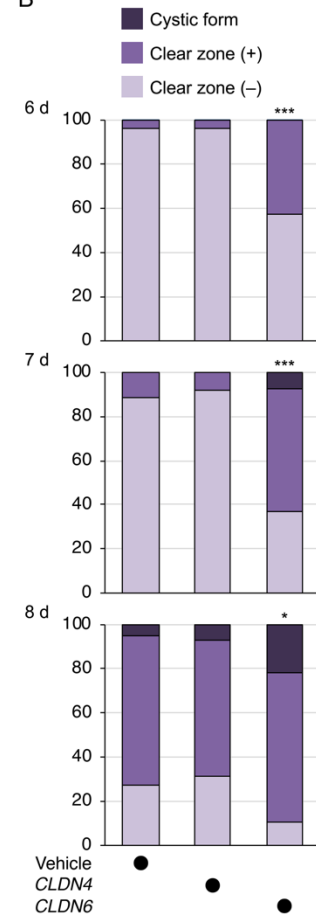


Fig. S12. Amino acid sequences of the first half of C-terminal cytoplasmic domains in mouse CLDNs. (A) Tyrosine residues corresponding to Y196 and Y200 in CLDN6 are indicated in red. (B) Mouse ES cells were transfected with mock, CLDN4 and CLDN6 expression vectors, and EBs were cultured for eight days, followed by categorization of their morphological appearance. All values were compared with those in control values. * $P < 0.05$; *** $P < 0.001$.

Table S1. List of antibodies.

| Antibodies | Host | Source | Identifier | IP | IB | IHC |
|-----------------------------|--------|--------------------------------|-------------|-----------|----------|-------|
| AKT | rabbit | Cell Signaling Technology | 4691S | | 1:1,000 | |
| β Actin | mouse | Thermo Fisher Scientific | A5441 | | 1:10,000 | |
| β Actin | rabbit | Thermo Fisher Scientific | A2103 | | 1:4,000 | |
| Claudin-6 | rabbit | Immuno-Biological Laboratories | 18865 | 2 μ g | 1:2,000 | 1:200 |
| Claudin-6 | goat | Santa Cruz Technology | sc17669 | | | 1:100 |
| Claudin-7 | rabbit | Immuno-Biological Laboratories | 18875 | | 1:1,000 | |
| E-cadherin | mouse | Becton Dickinson Bioscience | 610182 | | 1:2,000 | 1:200 |
| EBP50 | rabbit | Affinity Bio Reagents | PA-1-090 | | 1:2,000 | |
| Ezrin | rat | Sanko Junyaku | AB01006 | | 1:2,000 | 1:200 |
| FLAG | mouse | MBL Life Science | M185-3L | 2 μ g | | |
| FLAG | mouse | Sigma | F3165 | | | 1:500 |
| FLAG (HRP-conjugated) | mouse | Sigma | A8592 | | 1:2,000 | |
| HA | rat | Roche | 11867423001 | 1 μ g | 1:1,000 | 1:100 |
| HNF4 α | rabbit | Santa Cruz Biotechnology | sc6556 | | 1:1,000 | |
| NCoR | rabbit | Millipore | ABE251 | 1 μ g | | |
| Occludin | rabbit | LifeSpan BioScience | LS-B2187 | | 1:1,000 | |
| Occludin | mouse | Thermo Fisher Scientific | OC-3F10 | | | 1:100 |
| PI3K (55) | rabbit | Cell Signaling Technology | 11889S | | 1:1,000 | |
| Phospho-Tyrosine | mouse | Santa Cruz Technology | Sc-508 | 2 μ g | 1:1,000 | 1:100 |
| Phospho-AKT | rabbit | Cell Signaling Technology | 4060S | | 1:1,000 | |
| Phospho-PI3K (85/55) | rabbit | Bioss | bs-3332R | | 1:1,000 | |
| Phospho-SFK (Tyr416) | rabbit | Cell Signaling | 2101 | | 1:1,000 | 1:100 |
| Radixin | rat | Sanko Junyaku | AB01007 | | 1:2,000 | |
| SFK | rabbit | Millipore | 05-1461 | | 1:1,000 | |
| ZO-1 (α + variant) | rat | Santa Cruz Technology | sc33725 | | 1:1,000 | 1:100 |
| goat IgG (Alexa Fluor488) | donkey | Thermo Fisher Scientific | A-11055 | | | 1:200 |
| mouse IgG (HRP) | goat | Dako | P0447 | | 1:4,000 | |
| mouse IgG (Alexa Fluor488) | goat | Thermo Fisher Scientific | A-11029 | | | 1:200 |
| mouse IgG (Alexa Fluor594) | goat | Thermo Fisher Scientific | A-11032 | | | 1:400 |
| mouse IgG (Alexa Fluor647) | goat | Thermo Fisher Scientific | A-21235 | | | 1:200 |
| rabbit IgG (HRP) | goat | Dako | P0448 | | 1:2,000 | |
| rabbit IgG (Alexa Fluor488) | goat | Thermo Fisher Scientific | A-11034 | | | 1:200 |
| rabbit IgG (Alexa Fluor594) | goat | Thermo Fisher Scientific | A-11012 | | | 1:400 |
| rat IgG (HRP) | goat | Dako | P0450 | | 1:2,000 | |
| rat IgG (Alexa Fluor594) | goat | Thermo Fisher Scientific | A-11007 | | | 1:200 |

Table S2. List of siRNAs.

| Gene | Sense | Antisense |
|----------------------|---------------------------|---------------------------|
| <i>Cldn6</i> RNAi #1 | AAGAUUUGCAGACCAGUAGAGGCCA | UGGCCUCUACUGGUCUGCAAUCUU |
| <i>Cldn6</i> RNAi #2 | CCCACUCUAUCAUCCAGGACUUCUA | UAGAAGUCCUGGAUGAUAGAGUGGG |
| <i>Hnf4a</i> RNAi #1 | AUGUGUUCUUGCAUCAGGUGAGGGU | ACCCUCACCUGAUGCAAGAACACAU |
| <i>Hnf4a</i> RNAi #2 | UACAUGUGGUUCUCCUCACGCUCC | GGAGCGUGAGGAAGAACCACAUGUA |

Table S3. List of primers.

| Gene | Forward | Reverse | Cycles | Ref. |
|------------------------------|---------------------------------|---------------------------------|--------|---------------------|
| <i>Cldn6</i> | CGGCAACAGCATCGTCGTG | TCTTGGTGGGATATTCGGAGG | 18-20 | Kubota et al., 2001 |
| <i>Cldn6</i> (endogenous) | CCCTCCGAATATCCCACCAAGAATT | AGTGGAACAAACCCTAGGGACAGA | qPCR | This paper |
| <i>Cldn7</i> | GCGACAACATCATCACAGCC | CCTTGGAGGAATTGGACTTGG | 28-30 | Kubota et al., 2001 |
| <i>36b4</i> | GTGTACTCAGTCTCCACAGA | CAGCTCTGGAGAAACTGCTG | 18-20 | Kubota et al., 2001 |
| <i>Cyp26a</i> | GGAAACATTGCAGATGGTGC | CCCAAACAGATGCGTCTTGT | qPCR | This paper |
| <i>Rarb</i> | GCACCGGCATACTGCTCAAT | CAAACGAAGCAGGGCTTGT | qPCR | This paper |
| <i>Hnf4a</i> | AATGTGCAGGTGTTGACCAT | CTTCTCACGCTCCTCCTGA | qPCR | This paper |
| <i>Cldn6</i> ChIP 1 | TCAGGAAACCGTGGTGTCTGAGCTTGTGTT | ATAGAGGCAGGGATGTTGAGAGTGGAGGCA | 35-40 | This paper |
| <i>Cldn6</i> ChIP 2 | CTCAGATCCTCCACTCTCTCCATACCCA | ACTGCTTACTGGTGTGAGACAGTCTCGTAA | 35-40 | This paper |
| <i>Cldn6</i> ChIP 3 | GACTTCTTACCTTCTTGAGAATTTCTGCC | GCTTTGACTTGGCTCCCTACCTCTCTTTCA | 35-40 | This paper |
| <i>Cldn6</i> ChIP 4 | GAGGAGCTGAAAGTCTCGTCCATCAGGG | AATTCTCAAGAAGTAAGAAGTCTGGAGCC | 35-40 | This paper |
| <i>Cldn6</i> ChIP 5 | AAGACCTGAGGTGCCAGAGGGTGGGGCTG | GGTCCAGACCATCGAAGTCTACAAGCATGA | 35-40 | This paper |
| <i>Cldn6</i> ChIP 6 | TTTAAAACCCCTATCCAAAACACAAGCAT | GACTTAGCCAGGTATGTCTTCTTTGTCTTC | 35-40 | This paper |
| <i>Cldn6</i> ChIP NC | CCAAAGTCCGAGGTTTACCCTCGTCTGAGC | AGCAGACAGTTCTTGCCTCGGGACCGGCAA | 35-40 | This paper |
| <i>Rarb</i> ChIP 1 | TTCAATTATGCTTTGTAAGGAAGCCAGTA | GTGCTCTCAGGTGCCCTTTCTCCAGGAGGCT | 35-40 | This paper |
| <i>Rarb</i> ChIP 2 | CAGGAGCACTCTTCCAGCGTGGCAGGCCTTG | CTGCTGATGCACCAGAATGCATGCAAGTGA | 35-40 | This paper |
| <i>Rarb</i> ChIP 3 | CCATTTGTCTGATGCTGACAGAAGTCTGAA | GTGAGTATCAAGTAGTCCCTCGGTCCTTA | 35-40 | This paper |
| <i>Rarb</i> ChIP 4 | GCCTCCTATGGCAGACTCTCAAATATCTCA | TGGGAGTTTCTGCACATGCCTGTTTAGGAT | 35-40 | This paper |
| <i>Rarb</i> ChIP 5 | TCTCCTCTGGTATTTGAATGCCAAGACA | AGAAAATGTGAGCAAGTCCAATGAAATCCT | 35-40 | This paper |
| <i>Rarb</i> ChIP 6 | ATAAACAGATGAAAGTTCCTTCTCGGGCT | GGGACTACTTCAAATGCCTTCTCCACTACA | 35-40 | This paper |
| <i>Rarb</i> ChIP NC | TCTAGCTGAGGTGGATAAGGAAGGTTGCT | TGATTGAGTGAACCTGTGAGAGTACAGCA | 35-40 | This paper |
| <i>Hnf4a</i> ChIP 1 | CTCACTGTTTGTCTAGGTTGAATGGTCTGT | TCCCACCTCTCTATCTTTCTACCCACAA | 35-40 | This paper |
| <i>Hnf4a</i> ChIP 2 | ACTCTCGGGAGGCTGAGGCAGAGGGAAGT | GGAGGGCACAGATGTCAGATCCACGCACAC | 35-40 | This paper |
| <i>Hnf4a</i> ChIP 3 | TGCTCCAGAAAGTTCGCCACACATAGGA | ATAAACCTAGGGCTTCAAGTATGCTAGGCA | 35-40 | This paper |
| <i>Hnf4a</i> ChIP 4 | GGAGTTGATTCTCTTCCACAGGCTCCAGGT | TAGCCTCAGGTGCTTTAACCACAGAGCCA | 35-40 | This paper |
| <i>Hnf4a</i> ChIP 5 | CATTGGAAGCTAAGCAATAGTGCAGGCTAT | TGCATCATGGGAAGGGACACGCAAAGCAGA | 35-40 | This paper |
| <i>Hnf4a</i> ChIP 6 | TTACAGATGGTGTGAGCCACCCTGTGGTT | ATCCTCAGACACTCAGAAGAGGGCATAAGA | 35-40 | This paper |
| <i>Hnf4a</i> ChIP NC | TGAGAATTCTGCCAATTTCTGAGTATATCT | AAATAATCAGACTTTTCGGGGTCTGCTGGA | 35-40 | This paper |
| <i>BRF1</i> | AAGATGCTTCAGGAGACGGTG | CCTCTGTTCCCGCAGGTACT | qPCR | This paper |
| <i>GAPDH</i> | GTCTCCTCTGACTTCAACAGCG | ACCACCCTGTGTGTAGCCAA | qPCR | This paper |
| <i>GRK3</i> | ATAATGAGGAAGACCGCCTTTGC | GACTTTGTACGTGTTCTACAGCTTGC | qPCR | This paper |
| <i>MOV10</i> | CACAGTGACTTCTTACCTGAAGC | AGCTCCCTGTCAAGTTGGT | qPCR | This paper |
| <i>PLEKHA6</i> | GACCAGGATATCAACGCCACC | CGAATATCTGGGCATCTGTGA | qPCR | This paper |

References

56. Chiba H, Chambon P, Metzger D (2000) F9 embryonal carcinoma cells engineered for tamoxifen-dependent Cre-mediated site-directed mutagenesis and doxycycline-inducible gene expression. *Exp Cell Res* 260(2):334–339.
57. Van Itallie CM, Betts L, Smedley JG III, McClane BA, Anderson JM (2007) Structure of the Claudin-binding Domain of Clostridium perfringens Enterotoxin. *J Biol Chem* 283(1):268–274.
58. Uchida H, et al. (2010) A claudin-4 modulator enhances the mucosal absorption of a biologically active peptide. *Biochem Pharmacol* 79(10):1437–1444.
59. Ishizaki T, et al. (2003) Cyclic AMP induces phosphorylation of claudin-5 immunoprecipitates and expression of claudin-5 gene in blood–brain-barrier endothelial cells via protein kinase A-dependent and -independent pathways. *Exp Cell Res* 290(2):275–288.
60. Delfosse V, et al. (2012) Structural and mechanistic insights into bisphenols action provide guidelines for risk assessment and discovery of bisphenol A substitutes. *Proc Natl Acad Sci USA* 109(37):14930–14935.